Available online at www.sciencedirect.com
ScienceDirect
Journal of Power Sources 160 (2006) 821–826
JOURNAL OF POWER SOURCES
www.elsevier.com/locate/jpowsour

Short communication

Morphological, structural and electrochemical analysis of sputter-deposited ceria and titania coatings for MCFC application

Valérie Albin [a], Leonardo Mendoza [a], Aurélie Goux [a], Armelle Ringuedé [a], Alain Billard [b], Pascal Briois [b], Michel Cassir [a,*]

[a] *Laboratoire d'Electrochimie et de Chimie Analytique, UMR 7575 CNRS, ENSCP, 11 rue Pierre et Marie Curie, 75231 Paris Cedex 05, France*
[b] *Laboratoire de Science et Génie des Surfaces (UMR 7570), Ecole des Mines, Parc de Saurupt, F 54042 Nancy Cedex, France*

Available online 6 June 2006

Abstract

In order to protect the MCFC nickel cathode, TiO_2 and CeO_2 coatings were prepared by DC reactive magnetron sputtering. These oxides are stable thermodynamically whatever the cathode or anode gaseous conditions. Good quality, dense and homogeneous coatings were obtained at thicknesses lower than 1 μm. The structure of the deposits, as analysed by XRD, was the expected one. In this work only dense nickel substrates were used. After their direct immersion in a Li_2CO_3–Na_2CO_3 carbonate eutectic at 650 °C, which can be considered as extremely corrosive conditions with respect to the usual MCFC conditions, the coatings were affected. TiO_2 coatings were transformed into Li_2TiO_3, in agreement with thermodynamic predictions; however, they became progressively unstable, which was probably due to a problem of mechanical adhesion rather than to solubility. The thinner was the deposit, the higher was its conductance and the closer to that of a pure Ni electrode was its electrocatalytic activity. CeO_2 coatings were stable in a ceria form and their adhesion was better even though not fully satisfactory. These first preliminary results are promising regarding the direct contact of the coatings with the corrosive carbonate melt, but the improvement of the adhesion is one of the major problems to solve.

Keywords: CeO_2; TiO_2; Coatings; Reactive magnetron sputtering; MCFC

1. Introduction

One of the main problems, apart from cost, in developing high temperature fuel cells such as molten carbonate fuel cell (MCFC) remains its too short life-time. The origin of this limitation is mainly due to the dissolution of the nickel cathode in the carbonates and to the slow corrosion of bipolar plates, in particular in the anode side [1,2]. In this work, we present the potential role of very thin protective oxide coatings versus the corrosive effect in the carbonates, as diffusion barriers at the cathode/electrolyte (or bipolar plate/anode interfaces in a forthcoming paper). TiO_2 deposits have already been considered as protective coatings of the stainless steels constituting MCFC bipolar plates [2–6], but, as far as we know, never in the case of the nickel cathode. CeO_2 has also been analysed for different uses in MCFC applications: as additive for the Ni cathode [7–9], cathode coating [10], anode [11], anode coating [12,13] or anode matrix material [14]. Reactive magnetron sputtering, a physical directional deposition technique allowing the elaboration of very thin and dense oxide layers, was used to deposit CeO_2 and TiO_2-based layers. According to previous studies, TiO_2 and CeO_2 compounds seem to be stable in molten carbonate in both anode and cathode MCFC environment. Some progress has already been achieved in our laboratory [15–19]. A thorough fundamental study of the behaviour of titanium and cerium species has been fully realised, including thermodynamic predictions, electrochemical in situ measurements, solubility determinations and surface characterisation after treatment (structure, morphology, oxidation degrees) by XRD and SEM/EDS techniques. The stable species in molten carbonates are Li_2TiO_3 and CeO_2 whatever the conditions (anode, or cathode standard conditions). This work will only be focused on titanium or cerium oxides deposited on dense nickel substrates, used as a reference substrate. Works using doped titanium or cerium oxides and other substrates such as porous nickel electrodes and stainless steels are in progress.

* Corresponding author.
E-mail address: michel-cassir@enscp.fr (M. Cassir).

0378-7753/$ – see front matter © 2006 Elsevier B.V. All rights reserved.
doi:10.1016/j.jpowsour.2006.04.066

2. Experimental

Electrochemical measurements were carried out using a Princeton Applied Research (PAR) Model 263A potentiostatic system, with a three electrodes electrochemical configuration: (1) working electrode: sample itself connected to a gold wire; (2) counter-electrode: gold wire; (3) reference electrode: silver wire dipped into an Ag_2SO_4 (10^{-1} mol kg^{-1}) saturated eutectic melt in an alumina cylinder sealed by a porous alumina membrane. Impedance measurements were performed using a Voltalab 30 generator, coupled with a Volta Master 3.0 software. The ac signal amplitude was of 5 mV with respect to OCP, low enough to respect the system linearity. All the diagrams were recorded from 10^5 to 1 Hz.

Ceria and titania coatings were sputter-deposited on Nickel substrates by direct current sputtering of a metallic Ce or Ti target in argon–oxygen reactive mixtures. The experimental device is a 40 l sputtering chamber pumped down via a turbo-molecular pump allowing a base vacuum of about 10^{-4} Pa before refilling with argon to reach a pressure of 0.59 Pa. The substrates are positioned facing the target on a substrate holder at a draw distance (D_{T-S}) of about 60 mm. The target (Ce or Ti), mounted on an unbalanced magnetron, was powered by a pulsed DC supply (Advanced Energy Pinacle) equipped with a Sparc-Le 20 pulse unit operating in DC (Ti) or in active arc (Ce) mode. For all the experiments, the discharge current was maintained at a constant value of 0.7 A. The flow rates of argon and oxygen are controlled by MKS flowmeters and the total pressure is measured using a MKS Baratron gauge. In order to ensure the stoichiometry of all the coatings, the oxygen flow rate was set at 8 sccm, yielding a total pressure of about 0.68 Pa. Before the deposition stage, all the samples were cleaned in a boiling dichloromethane solution, then treated in an ultra-sound bath, rinsed in ethanol and dried with hot air.

The thickness of the films was also measured by the step method, with a Talysurf profilometer, allowing an accuracy of the measurements of about 40 nm. The morphology and composition of the samples were examined by scanning electron microscopy (SEM), provided by JEOL T330A, associated to energy-dispersive spectroscopy (EDS). XRD experiments were carried out with a Siemens D5000 type diffractometer using a Co $K_{\alpha 1}$ radiation ($\lambda = 1.789$ Å) and a back graphite monochromator. The diffraction pattern was scanned by steps of 0.02° (2θ) with a fixed counting time (2.3 s) between 16° and 80°. The electrolyte is constituted by Li_2CO_3–Na_2CO_3 eutectic, operating at 650 °C. After reaching the melt equilibrium (about 48 h), the exposure time selected was variable. The standard gaseous cathode atmosphere is composed by 70% air and 30% CO_2. After exposure to the carbonate melt, for the ex situ characterisations (XRD, SEM/EDS), the samples were rinsed in ultra-pure water, baked at 100 °C for about 1 h in air, and stored in boxes.

3. Results and discussion

3.1. TiO_2 deposits on nickel

Fig. 1 shows the SEM micrographs of TiO_2 coatings on dense nickel substrates, with thicknesses varying from 200 to 800 nm. These deposits are well-covering and dense and no cracks can be observed. However, after 8 h of direct exposure to the carbonate melt in the usual cathode atmosphere, important changes are detectable. In the case of the 200 and 400 nm coatings, the surface is quite damaged with a significant splitting of the deposits. This evolution is less pronounced for the two thicker deposits, 600 and 800 nm. Semi-quantitative EDS measurements show that only 20% and 30% of the titanium remains for the 200 and 400 nm coatings, respectively, whereas this ratio is about 60% and 70% for the 600 and 800 nm deposits, respectively.

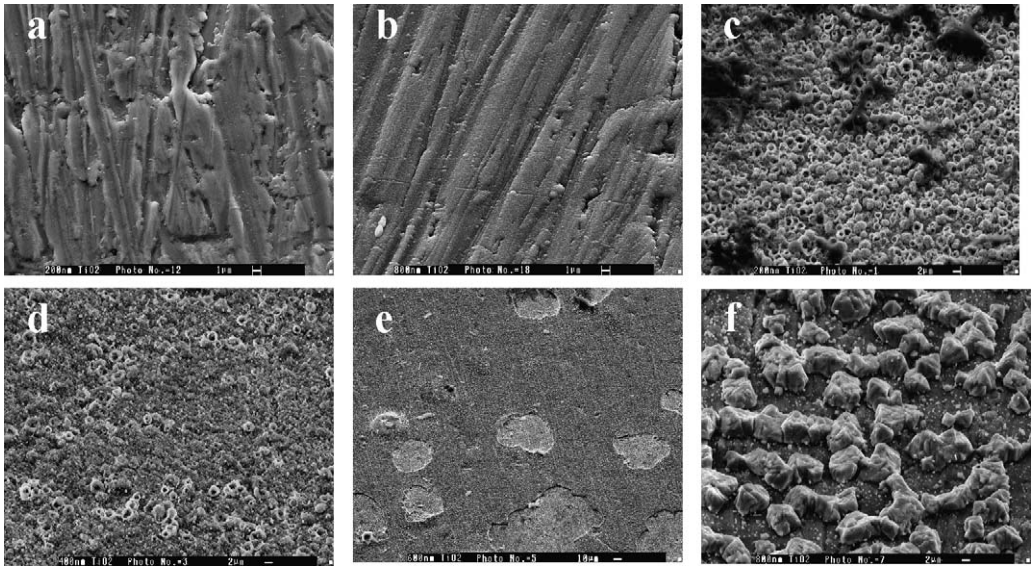

Fig. 1. SEM micrographs of TiO_2 deposited on Ni. Before and after immersion during 8 h in Li_2CO_3–Na_2CO_3 (52–48 mol.%) at 650 °C under air/CO_2 (70/30). (a) Before immersion (thickness 200 nm), (b) before immersion (800 nm), (c) after immersion (200 nm), (d) after immersion (400 nm), (e) after immersion (600 nm), and (f) after immersion (800 nm).

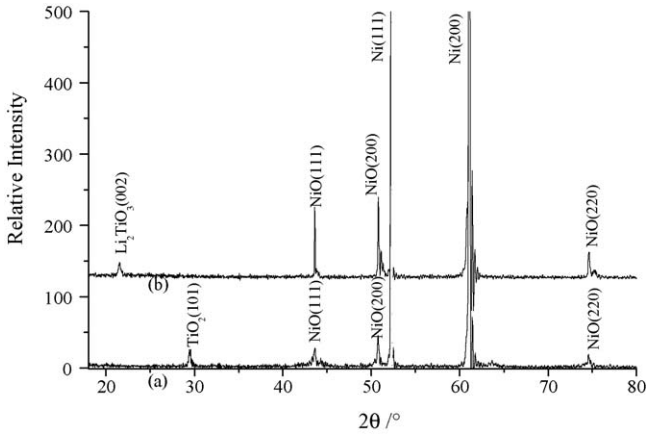

Fig. 2. XRD diffractograms obtained on pellets of a TiO_2-coated nickel foil (2 cm^2), before and after 60 min. of immersion in Li_2CO_3–Na_2CO_3 (52–48 mol.%) at 650 °C under air/CO_2 (70/30). (a) TiO_2 coating, thickness 0.8 μm, after thermal treatment during 4 h under air. (b) Same deposit after an hour of immersion in the melt.

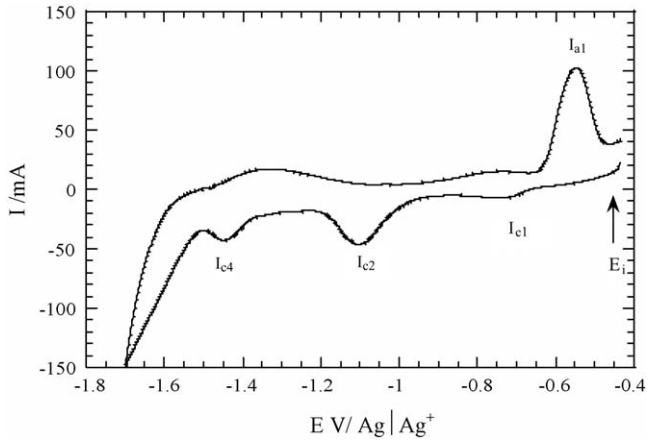

Fig. 4. Cyclic voltammogram at 20 mV s^{-1} of a TiO_2-coated (thickness 600 nm) nickel foil (2 cm^2) in Li_2CO_3–Na_2CO_3 (52–48 mol.%) at 650 °C under air/CO_2 (70/30).

It should be noted that all the as-deposited coatings are amorphous whatever their thickness. Therefore, XRD measurements were realised after a thermal treatment at 500 °C during 4 h under air, as can be seen in Fig. 2 for a 0.8 μm-thick coating. This allowed us to confirm the presence of titanium oxide. After an immersion of 1 h, Li_2TiO_3 (0 0 2 line) was identified on the 800 nm-thick sample. For all the other thicknesses, only Ni and NiO were detected, because, from the one hand, the XRD analysis depth is bigger than the deposits thicknesses and, by the other hand, as was already seen because of the mechanical spilling of the coatings.

OCP (open circuit potential) of the different TiO_2 coatings was followed during 8 h in the molten carbonate. Fig. 3 shows that the starting potential is −0.9 V/Ag|Ag^+, value already observed [20], studying the behaviour of NiTi alloy in the same experimental conditions. This potential probably corresponds to the oxidation of TiO_2 into Li_2TiO_3, according to: $TiO_2 + 2Li^+ + CO_3^{2-} \rightarrow Li_2TiO_3 + CO_{2(g)}$.

Afterwards, the potential increases until reaching the potential of a pure Ni electrode. This last step tends to get larger with the thickness of the TiO_2 coating. The thinnest coatings seem more advantageous from the electrocatalytic viewpoint, because their behaviour is closer to that of Ni, the usual cathode material. But this apparent advantage could be due to their instability in the carbonate melt and to the presence of the Ni substrate. Beyond 400 nm, no important influence on the potential evolution can be noted.

Cyclic voltammograms were recorded at a scan rate of 20 mV s^{-1}, different immersion times and a start potential which is the OCP, in order to understand better the electrochemical behaviour of the deposits. Fig. 4 corresponds to a deposit of 0.6 μm after 1 h of immersion in the carbonate melt. The characteristic peaks of NiO/Ni system, fully depicted by Belhomme et al. [21], are not observed, confirming that nickel is well protected by the titanium oxide, in a Li_2TiO_3 form. Therefore, peaks I_{c1}, I_{c2}, I_{c4} and I_{a1} can be due to the presence of titanium species. Thermodynamically, the Li_2TiO_3 present on the surface is stable and should not be oxidised or reduced; however according to Chauvaut and Cassir [17], Li^+ (and also probably Na^+) proceed-

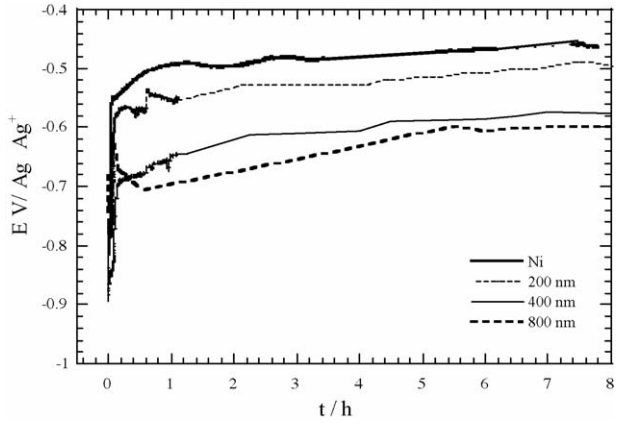

Fig. 3. OCP time-evolution of TiO_2 coatings, with different thicknesses, on Ni (2 cm^2) and of a pure Ni electrode in Li_2CO_3–Na_2CO_3 (52–48 mol.%) at 650 °C under air/CO_2 (70/30).

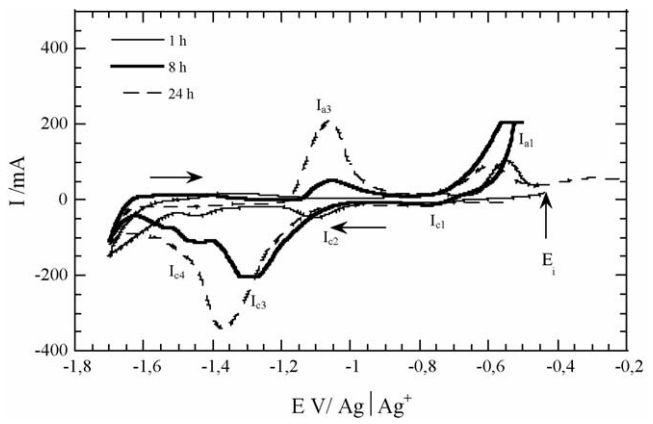

Fig. 5. Cyclic voltammograms at 20 mV s^{-1} of a TiO_2-coated (thickness 600 nm) nickel foil (2 cm^2) with different immersion duration in Li_2CO_3–Na_2CO_3 (52–48 mol.%) at 650 °C under air/CO_2 (70/30).

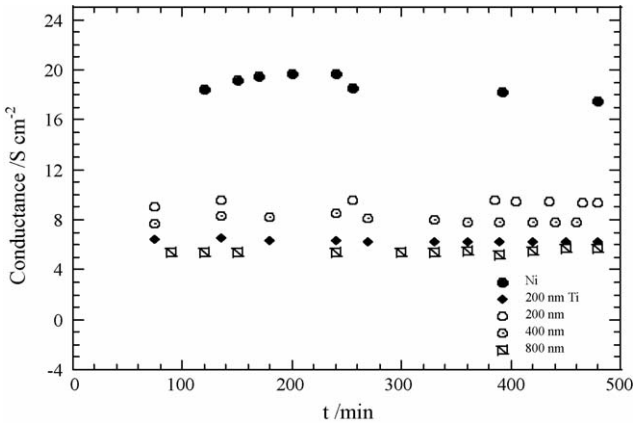

Fig. 6. Conductance of a nickel foil and TiO_2-coated nickel foils, at different thicknesses vs. the immersion duration in Li_2CO_3–Na_2CO_3 (52–48 mol.%) at 650 °C under air/CO_2 (70/30).

ing from the electrolyte can be intercalated within the Li_2TiO_3 monoclinic structure, which possess at least two octahedral and two tetrahedral sites. The peaks mentioned could correspond to different intercalation–deintercalation processes due to the presence of compounds in a $Li_{2+x}TiO_3$ form. Experimental evidence has already been given for this phenomenon:

$$Li_2Ti^{IV}O_3 + xLi^+ + xe^- \rightarrow Li_{2+x}Ti_{1-x}{}^{IV}Ti_x{}^{III}O_3.$$

Fig. 5 shows the cyclic voltammograms evolution with respect to the immersion time. It is clear that a new system I_{a3}/I_{c3} becomes progressively predominant, with respect to the other phenomena. It most probably represents the nickel redox system: $Ni + CO_3{}^{2-} \rightarrow NiO + CO_2 + 2e^-$ (in a simplified way, knowing that NiO is under a $Li_xNi_{1-x}O$, with $x = 0.002$ [22]. According to the literature [21], this system appears, in principle, at -1.2 V/Ag|Ag^+; the slight potential shift can be due to a lower kinetics in our present case. The peaks, initially present after 1 h immersion, fully disappeared after 24 h of immersion in the melt, showing that the surface of the sample is mainly recovered by lithiated nickel oxide and that the TiO_2 coating fell into the melt.

It was also shown that the conductance, obtained by impedance spectroscopy, was significantly lower for the coated samples than that for pure nickel (stabilised at about 20 S cm^{-2} after few hours): 1/3 for the thicker coating (800 nm) and 1/2 for the thinner one (200 nm). This can be clearly observed in Fig. 6. It is also interesting to note that the conductance of Ni pellet recovered with a thin film of titanium (200 nm) is significantly lower than that of a Ni pellet recovered with TiO_2 (200 nm). This difference can be due to the fact that in the first case (Ti-coated Ni), nickel is recovered by a double layer: an internal one, TiO_2, and an external one, Li_2TiO_3 [16,23], with the following oxidation mechanism: $Ti + O_2 \rightarrow TiO_2$ and $TiO_2 + 2Li^+ + CO_3{}^{2-} \rightarrow Li_2TiO_3 + CO_2$.

3.2. CeO_2 deposits on nickel

The same study was realised on CeO_2 coated nickel. Fig. 7 show the SEM micrographs of CeO_2-coated nickel, with two thicknesses, 0.6 and 1.2 μm, before and after immersion in the carbonate melt.Before immersion, the deposit, constituted by CeO_2, is well-covering, dense and homogeneous and does not

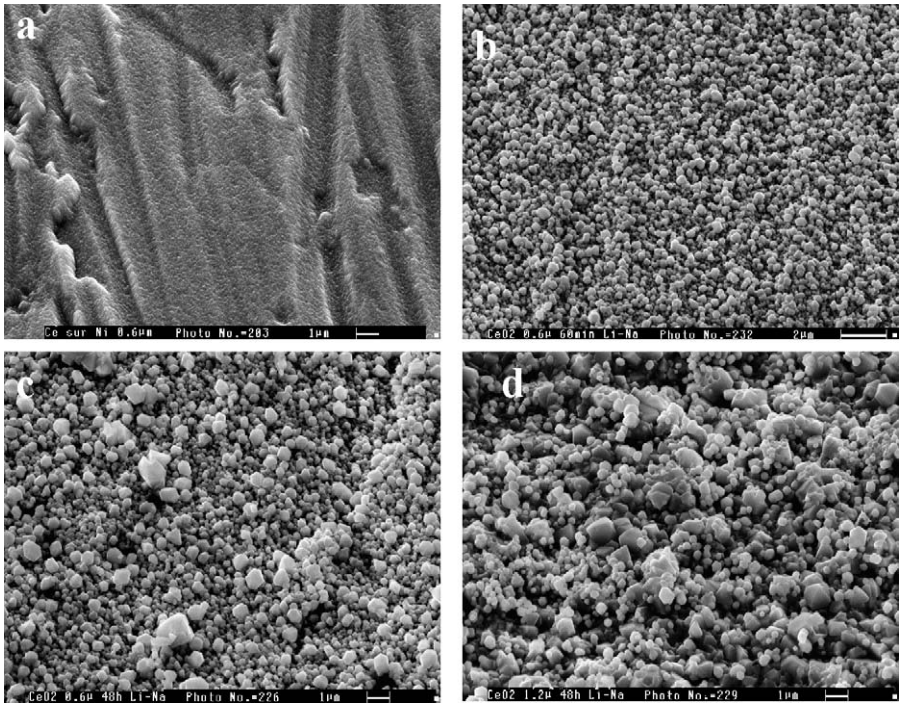

Fig. 7. SEM micrographs of CeO_2 deposited on dense Ni. Before and after immersion in Li_2CO_3–Na_2CO_3 (52–48 mol.%) at 650 °C under air/CO_2 (70/30). (a) CeO_2 deposited on a Ni foil. Thickness 600 nm. (b) Same deposit after 1 h in the melt. (c) Same deposit after 48 h in the melt. (d) CeO_2 deposited on a Ni foil. Thickness 1.2 μm. After 48 h in the melt.

Table 1
Atomic rate of Ce, Ni and O according to the EDS analysis of Ni foils recovered by a 600 nm CeO_2 coating, before and after immersion in Li_2CO_3–Na_2CO_3 (52–48 mol.%) at 650 °C under air/CO_2 (70/30)

Immersion time (h)	Ce (at.%)	Ni (at.%)	O (at.%)
0	21	9	70
1	19	19	62
48	13	26	61

present apparent cracks. After one hour immersion, the nickel surface is recovered by well-distributed and uniform grains (of about 50 Å). After 48 h, the grain size slightly increases and distribution is less uniform, because some of the grains have fallen in the carbonate melt. Table 1 shows the results of EDS analysis on a 600 nm coating. After 48 h of exposure to the carbonate bulk, the amount of remaining cerium is about 60% of the initial amount, which means that, although the mechanical stability of the coating is not perfect, this kind of deposition process is interesting and can be optimised.

The XRD diffractogram, described in Fig. 8 shows very clearly the predominant presence of the (1 1 1), (2 0 0), (2 2 0), (3 1 1) and (2 2 2) CeO_2 characteristic lines, which was not the case for the TiO_2 coating. Only metallic nickel lines can be observed: Ni (1 1 1) and Ni (2 0 0). The crystalline character of the CeO_2 deposit is favoured by the immersion in molten carbonates.

The OCP time-evolution of a CeO_2 (0.6 μm)-coated nickel pellet is depicted in Fig. 9. The starting potential is −0.9 V/Ag|Ag^+; then it increases rapidly during the first minutes and remains constant at a value fluctuating around −0.5 V/Ag|Ag^+. This behaviour is complex due to the fact that Ce(IV) is in principle the only stable cerium species in the carbonate melt and that there is no possibility to reduce it into another stable species. The nickel substrate itself might be oxidised and could get involved to fix the potential. Different phenomena could be taken into account for the OCP establishment:

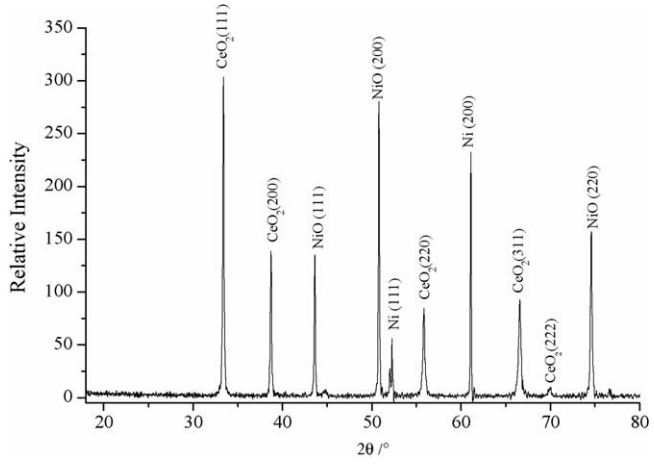

Fig. 8. XRD diffractogram obtained on a pellet of CeO_2 (0.6 μm)-coated nickel foil (2 cm^2), after 60 min of immersion in Li_2CO_3–Na_2CO_3 (52–48 mol.%) at 650 °C under air/CO_2 (70/30).

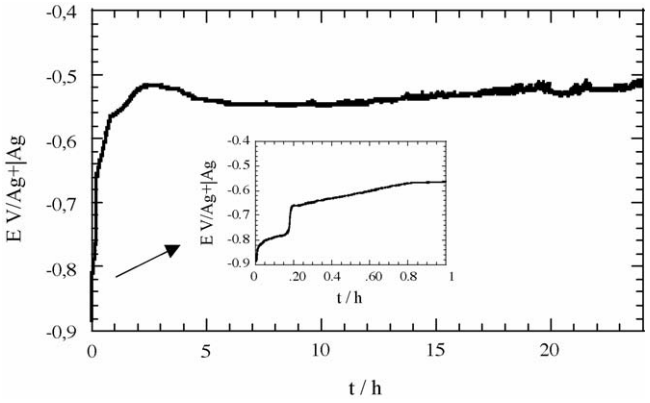

Fig. 9. OCP time-evolution obtained on a pellet of CeO_2 (0.6 μm)-coated nickel foil (2 cm^2), after 60 min of immersion in Li_2CO_3–Na_2CO_3 (52–48 mol.%) at 650 °C under air/CO_2 (70/30).

- an equilibrium could be established between non-stoechiometric cerium oxides: CeO_{2-x} (x value between 10^{-4} and 10^{-3}) [24], modifying the deposit conductivity and electrocatalytic properties;
- a chemical insertion of small amounts of alkali cations could modify the CeO_2 properties [25];
- a morphological evolution (increase in the porosity, grain size variations) during the immersion in the carbonate melt;
- the presence of nickel and its progressive oxidation can progressively become predominant.

After 24 h in the melt, OCP is close to that of a bare Ni pellet, which indicates that CeO_2 might have comparable electrocatalytic properties with respect to Ni.

4. Conclusion

TiO_2 and CeO_2-based coatings are interesting materials for MCFC, knowing that they are theoretically stable in the molten carbonate anode and cathode conditions. Even though the thermodynamic conditions are favourable to the stability of these coatings, the remaining problems are their adhesion and their mechanical stability. The layers obtained by sputtering are of good quality, but after immersion the TiO_2 coating is not stable and further optimisation is required. In the case of CeO_2, the results are promising and this kind of material presents a real interest. However, a serious problem of adhesion remains after long periods of immersion in the carbonate melt.

A specific effort should be undertaken to favour the adhesion of the coatings to the substrates and reinforce their mechanical stability. Several solutions should be exploited in the next works:

- use of a bond layer between the ceria-based coatings and the SS substrate, reducing the mechanical stress and thermal dilatation;
- adapt the intrinsic stress of the coatings to accommodate its differential thermal expansion relatively to the substrate;
- use of another deposition technique, i.e. ALD (atomic layer deposition), which allows to obtain very dense layers elabo-

rated monoatomic layer by monoatomic layer, with the specific advantage of being non-directional;
- conditioning the surface of the SS substrate by shot blasting.

The present work shows the interest of using protective coatings based on TiO_2 and CeO_2; nevertheless, an important effort for improving the coatings adhesion is necessary and, most particularly, in the case of titanium oxide. Cerium oxide coatings seem more promising and work is in progress on this oxide, pure or doped both on dense and porous substrates.

References

[1] J.P.T. Vossen, PhD Thesis, Netherlands Energy Research Foundation ECN, The Netherlands, 1994.
[2] M. Keijzer, K. Hemmes, P.J.J.M. Van Der Put, J.H.W. de Wit, J. Schoonman, Corros. Sci. 39 (1997) 483–494.
[3] R.C. Makhus, E. Bullock, A.H.H. Janssen, M. Cassir, Int. Patent, WO0021152, 2000.
[4] G. Liu, M. Li, Y. Zhou, Y. Zhang, J. Eur. Ceram. Soc. 23 (2003) 1957–1962.
[5] C.L. Zeng, W.T. Wu, Corros. Sci. 44 (2002) 1–12.
[6] F.J. Perez, D. Duday, M.P. Hierro, C. Gomez, A. Agüero, M.C. Garcia, R. Muela, A. Sanchez Pascual, L. Martinez, Surf. Coat. Technol. 161 (2002) 293–301.
[7] M.J. Escudero, T. Rodrigo, L. Daza, Catal. Today 107–108 (2005) 377–387.
[8] L. Daza, C.M. Rangel, J. Baranda, M.T. Casais, M.J. Martinez, J.A. Alonso, J. Power Sources 86 (2000) 329–333.
[9] J. Soler, T. González, M.J. Escudero, T. Rodrigo, L. Daza, J. Power Sources 106 (2002) 189–195.
[10] A. Hilmi, C.-Y. Yuh, US Patent Application 20,050,153,186, 2005.
[11] J.C. Trocciola, R.C. Nickols Jr., US Patent, 4,317,866, 1982.
[12] S.H. Hong, I.H. Oh, T.H. Hoon, S.W. Nam, H.Y. Ha, S.P. Yoon, J. Han, B.S. Kang, US Patent Application 2,030,096,155, 2003.
[13] S.W. Nam, S.P. Yoon, H. Devianto, J. Han, T.H. Lim, in: P. Taxil, C. Bessada, M. Cassir, M. Gaune-Escard (Eds.), Proc. of the Seventh Int. Symp. On Molten Salts Chem. and Technol., Toulouse, France, 2005, pp. 501–504.
[14] R.C. Nickols Jr., J.C. Trocciola, J.E. Rourke, US Patent 4,297,419, 1981.
[15] V. Chauvaut, M. Cassir, Y. Denos, Electrochim. Acta 43 (1998) 1991–2003.
[16] V. Chauvaut, E. Duval, B. Malinowska, M. Cassir, P. Marcus, J. Mater. Sci. 34 (1999) 2015–2022.
[17] V. Chauvaut, M. Cassir, J. Electroanal. Chem. 474 (1999) 9–15.
[18] V. Chauvaut, V. Albin, H. Schneider, M. Cassir, H. Ardelean, A. Galtayries, J. Appl. Electrochem. 30 (2000) 1405–1413.
[19] M. Cassir, V. Chauvaut, A. Alfarra, V. Albin, J. Appl. Electrochem. 30 (2000) 1415–1420.
[20] C. Belhomme, PhD Thesis, University of Paris VI (ENSCP), France, 2000.
[21] C. Belhomme, J. Devynck, M. Cassir, J. Electroanal. Chem. 545 (2003) 7–17.
[22] C. Belhomme, M. Cassir, C. Tessier, E. Bertoumieux, Electrochem. Solid-State Lett. 3 (2000) 216–219.
[23] V. Chauvaut, PhD Thesis, University of Paris VI (ENSCP), France, 1998.
[24] J.P. Eberhart, Analyse Structurale et Chimique des Matériaux, Dunod, Paris, 1989.
[25] C. Yuh, R. Johsen, M. Farooque, H. Maru, J. Power Sources 56 (1995) 1–10.